

## MAGNETIC TOPOLOGY OF A NAKED SUNSPOT: IS IT REALLY NAKED?

A. SAINZ DALDA<sup>1</sup>, S. VARGAS DOMÍNGUEZ<sup>2,3</sup> & T. D. TARBELL<sup>4</sup>

<sup>1</sup> Stanford-Lockheed Institute for Space Research, Stanford University, HEPL, 466 Via Ortega, Stanford, CA 94305-4085, USA

<sup>2</sup> Departamento de Física, Universidad de Los Andes, A.A. 4976, Bogotá, Colombia

<sup>3</sup> Mullard Space Science Laboratory, University College London, Holmbury St Mary, Dorking, Surrey, RH5 6NT, UK and

<sup>4</sup> Lockheed-Martin Solar and Astrophysics Laboratory, Bld. 252, 3251 Hanover Street, Palo Alto, CA 94304, USA

*To appear in The Astrophysical Journal*

### ABSTRACT

The high spatial, temporal and spectral resolution achieved by Hinode instruments give much better understanding of the behavior of some elusive solar features, such as pores and naked sunspots. Their fast evolution and, in some cases, their small sizes have made their study difficult. The moving magnetic features, despite being more dynamic structures, have been studied during the last 40 years. They have been always associated with sunspots, especially with the penumbra. However, a recent observation of a naked sunspot (one with no penumbra) has shown MMF activity. The authors of this reported observation expressed their reservations about the explanation given to the bipolar MMF activity as an extension of the penumbral filaments into the moat. How can this type of MMFs exist when a penumbra does not? In this paper, we study the *full* magnetic and (horizontal) velocity topology of the same naked sunspot, showing how the existence of a magnetic field topology similar to that observed in sunspots can explain these MMFs, even when the intensity map of the naked sunspot does not show a penumbra.

*Subject headings:* Sun: magnetic topology — sunspots

### 1. INTRODUCTION

The so-called *Moving Magnetic Features* (hereafter MMFs) were discovered by Sheeley (1969) and Vrabec (1971) and described in detail by Harvey & Harvey (1973) and Vrabec (1974). From the early observations, they were associated with the moat (Vrabec 1974; Meyer et al. 1974; Brickhouse & Labonte 1988): an annular region surrounding the sunspot where the MMFs runaway from the penumbra towards the network. MMFs have been explained by an horizontal velocity field in the moat that drags the more horizontal, detached magnetic field lines from the bundle that forms the sunspot. Recently, MMFs have been observed coming from the mid-penumbra and entering the moat region, which is dominated by large outflows (Sainz Dalda & Martínez Pillet 2005; Ravindra 2006; Kubo et al. 2007). Sainz Dalda & Martínez Pillet (2005) averaged a temporal sequence of SoHO/MDI high-resolution magnetograms that revealed a transverse component of the magnetic field beyond the penumbra outer edge as an extension of the most horizontal penumbral filaments in the moat. High spatial resolution data have revealed a sea-serpent behavior of the more horizontal penumbral filaments as responsible for the bipolar magnetic structures in the mid-penumbra that become MMFs when they reach the moat (Sainz Dalda & Bellot Rubio 2008). All these results establish a link between MMF activity and the horizontal magnetic field component in the penumbra with the Evershed flow, as was suggested early on by Vrabec (1974).

One of the open questions about the moat is whether it exists or not around pores and naked sunspots<sup>1</sup>.

Vargas Domínguez et al. (2007, 2008) observed sunspots with different penumbral configurations and using *local correlation tracking* techniques (hereafter LCT) pointed out that the horizontal velocity flow is present in the part of the sunspot where penumbra exists. Vargas Domínguez et al. (2010) observed the horizontal flows around several pores. They did not find a moat around pores. On the contrary, they found an inflow region surrounding them. Bellot Rubio et al. (2008) analyzed the spectropolarimetric decay of a sunspot penumbra. They observed some finger-like structures remaining out of the naked sunspot after the penumbra disappeared. The presence or absence of these finger-like structures can be due to the evolutionary state of the (naked) sunspot. In our study we do not see these signatures, but the strength and the inclination of their magnetic field values in and out of the naked sunspot are very similar (see Figure 3 in Bellot Rubio et al. 2008). Here, we present a similar one-instance study of the magnetic topology of the naked sunspot observed by Zuccarello et al. (2009) (hereafter ZETAL09).

ZETAL09 found MMF activity around a naked sunspot, asking for a revision of the previous results that related this activity to the horizontal magnetic field. Their main conclusion is: ‘*The presence of bipolar MMFs in a naked spot indicates that current interpretation of bipolar MMFs, as extensions of the penumbral filaments beyond the sunspot outer boundaries, should be revised, to take into account this observational evidence*’.

In this letter, we use spectropolarimetric measurements to present a new perspective on these data. As results, the MMFs are again related to the horizontal magnetic field component of the (naked) sunspot, usually associated with the penumbra, but not necessarily.

or will have a penumbra during its life. A pore never develops a penumbra during its whole lifetime.

<sup>1</sup> We consider a pore and a naked sunspot to be different solar features. We understand a naked sunspot to be a solar feature that does not show a penumbra when it is observed, but that had

We also give a new interpretation of the LCT results that shows an horizontal velocity flow distribution in agreement with previous results.

## 2. DATA AS VIEWED FROM THE MAGNETIC FIELD

The AR NOAA 10977 was observed in the Fe I 6301 and 6302 Å lines from 16:25 to 16:47 UT on 5 December 2007 with the spectropolarimetric instrument SOT/SP (Tsuneta et al. 2008) on the Hinode satellite (Kosugi et al. 2007). This is the closest available in time to the data studied by ZETAL09 (14:06 to 15:48 UT). The spatial and spectral sampling were  $0''.32$  and  $22\text{ mÅ}$  respectively. At the observation time, the naked sunspot was located at heliographic coordinates  $(-12^\circ, -5^\circ)$ . To obtain the most accurate values of the physical parameters we have applied the SIR inversion code (Ruiz Cobo & del Toro Iniesta 1992) to the Stokes profiles. The calibrated profiles are easily obtained thanks to the data reduction tools mainly developed by B. Lites and available in the SOT *SolarSoft* package. Several inversions with different initializations were done. Here, we present one that represents a trade-off between the accuracy in inferred values (i.e., with smallest errors) and the degrees of freedom allowed in the inversion. Therefore, we have chosen a combination of degrees of freedom that shows the best fit between the observed and the inverted profiles and is compatible with a reliable atmosphere model. We have used a simple model with a magnetic component occupying the whole pixel (i.e., filling factor is 1.0) and a fixed stray light contribution of 15%. We have verified that an inversion with stray light as a free parameter does not introduce significant improvement in the output model; therefore we selected a high mean value in the studied region, and kept it fixed in the inversion presented here.

Figure 1 shows maps of the naked sunspot belonging to the AR NOAA 10977 after the calibration of the Stokes parameters (first row) and their inversion (second and third row). In the top row, we present the Stokes Intensity (with respect to the continuum intensity) map, the Mean Circular Polarization Degree map (hereafter MCPD map) and the Mean Linear Polarization Degree map (hereafter MLPD map). The former two maps were respectively calculated as  $MCPD = \int_{\lambda_0}^{\lambda_1} \frac{|V(\lambda)|d\lambda}{I(\lambda)}$  and  $MLPD = \int_{\lambda_0}^{\lambda_1} \frac{\sqrt{Q^2(\lambda) + U^2(\lambda)}}{I(\lambda)} d\lambda$ , being  $\lambda_0$  and  $\lambda_1$   $6302.27 \pm 0.02\text{ Å}$  and  $6302.70 \pm 0.02\text{ Å}$  respectively, i.e., a spectral range including the line Fe I 6302 Å. The MCPD is a good proxy for the unsigned vertical component of the vector magnetic field, while the MLPD is good for the transverse component of the vector magnetic field. In these maps we have overlaid the contours corresponding to the displayed magnitude. Thus, the intensity contour at level  $I/I_c = 0.8$  delimits the naked sunspot from the granulation. In this paper, we shall refer to this region as *photometric naked sunspot*, in the sense that its nature is uniquely described by the intensity magnitude. The contour at the MCPD map encloses the area where  $MCPD > 3.5\%$ . Similarly, the contours at MLPD map delimit the area where  $MLPD > 1\%$ . In these maps, the intensity contour is displayed (black) as reference. Notice that in the MLPD maps there is a contour inside the region delimited by the intensity con-

tour, which belongs to the MLPD contour. These three maps simply retrieved from the Stokes profiles offer us valuable information at a glance. The most obvious is the existence of an extended magnetic field beyond the photometric naked sunspot edge. Both the longitudinal and the transverse component of the magnetic field are present inside the photometric naked sunspot and beyond its intensity contour. However, although valuable, these maps are a rough approximation to the vector magnetic field: they can not tell us much about either the strength of the magnetic field or its *true* topology.

The second row of Figure 1 shows the strength (left), the vertical (center,  $B_{vert}$ ) and the horizontal (right,  $B_{hor}$ ) components of the magnetic field vector<sup>2</sup>. In the strength map, three contours have been overlapped, from the inner to the outer: the intensity contour (black), the contour for values where  $B_{vert} > 0.25\text{ kG}$  (white) and the contour for values where  $B_{hor} > 0.15\text{ kG}$  (white). The last two contours are respectively shown in the  $B_{vert}$  and  $B_{hor}$  maps.  $B_{vert}$  values drop from roughly  $1.10 \pm 0.07\text{ kG}$  at the edge of the photometric naked sunspot to  $0.25 \pm 0.03\text{ kG}$  at the position of the  $B_{vert}$  contour, which is roughly located  $1''$  outside of the intensity contour of the naked sunspot.  $B_{hor}$  values go from  $0.80 \pm 0.05\text{ kG}$  at the outer part of the photometric naked sunspot to  $0.15 \pm 0.03\text{ kG}$  at  $1.5''$  outside of the intensity contour where the  $B_{hor}$  contour is located on average.

Finally, the third row shows the inclination in the LRF (left), velocity along the line of sight (hereafter LOS, center) and temperature (right). In this row, all maps have been overlaid with the three contours (intensity,  $B_{vert}$  and  $B_{hor}$ ). At the center of the naked sunspot the inclination is  $180^\circ$ , i.e., the magnetic field is directed inward to the solar surface. The inclination of the magnetic field in the LRF roughly drops from  $140 \pm 4^\circ$  ( $50 \pm 4^\circ$  with respect to the local horizontal) to  $110 \pm 4^\circ$  ( $20 \pm 4^\circ$ ) out the photometric naked sunspot. The LOS velocity is upward or close to zero everywhere both the photometric naked sunspot and its surroundings: there is not any trace of Evershed flow, even though the position of the naked sunspot is far off the center of the solar disc. The temperature map shows a hot ring just between the intensity contour and  $B_{vert}$  contour. The temperature of this ring is roughly  $5.50 \pm 0.08\text{ kK}$ . It is hotter than the temperature of the photometric naked sunspot ( $4.00 \pm 0.03 - 5.00 \pm 0.05\text{ kK}$ ) but cooler than the most prominent granules in the studied area. We can see one granule located at map coordinates (2,10) with a temperature of  $5.50 \pm 0.03\text{ kK}$ . The other granule is located at map coordinates (12,3), and it shows a temperature similar to the former one but in this case the error is  $\pm 0.10\text{ kK}$ . On average, the temperature of this ring is slightly hotter than the granulation, but it is still cooler than the hotter granules shown in the map.

The values of both components of the magnetic field are stronger than the noise level, and the errors of the components and inclination of the vector magnetic field presented in this paper are only slightly higher than the maximum errors obtained by Gosain et al. (2010).

<sup>2</sup> Whereas the terms longitudinal and transverse are used for the projection of the magnetic field vector on the observation reference frame, the terms vertical and horizontal are used for the projection on the local reference frame (hereafter LRF).

They calculated an error value for vector magnetic field of a sunspot observed by Hinode-SOT/SP using both a Monte-Carlo approach and a Milne-Eddington inversion. The maximum values that they obtained were:  $\pm 50$  G for the field strength and  $\pm 3^\circ$  for the inclination. Therefore, our results look as reliable and consistent as other observations and inversions (see also result and errors in Bellot Rubio et al. 2008). To summarize, the topology of the (full) vector magnetic field of the observed naked sunspot has been revealed. We refer to this new vision of the naked sunspot as the *magnetic naked sunspot*.

### 3. DATA AS VIEWED FROM THE VELOCITY FIELD

In order to analyze the proper motions around the (naked) sunspot, we have selected the same SOT/BFI data used by ZETAL09 for applying LCT to compute the flow map of horizontal velocities. A total of 51 G-band images from 14:06 to 15:48 UT ( $\sim 2$  min cadence) were processed with standard *SolarSoft* routines and co-aligned at a sub-pixel level by cross-correlation over the entire FOV between subsequent pairs of images. A sub-sonic filter (velocity threshold of  $4 \text{ km s}^{-1}$ ) was used to eliminate p-modes resulting in a final time series of 46 images after apodization.

The LCT procedure was then applied by using a correlation tracking window of FWHM  $1''0$ . Two cases (Cases 1 and 2) of maps of horizontal velocities were generated. In the computed map for Case 1 (same as presented by ZETAL09) the velocity vectors have a predominant trend to the right, and the velocities closer to the right edge of the FOV are generally larger in magnitude. Figure 2 (top left panel) shows a clipped region of the FOV in the vicinity of the (naked) sunspot. In Case 2, the time series were first aligned with respect to a window enclosing the (naked) sunspot. By doing this, we neglect the proper (inherent) motion of the sunspot through the surrounding granulation, thus focusing on the plasma motions around the *anchored* sunspot. We detected shifts with respect to Case 1 of up to 26 and 10 pixels in the x and y directions respectively. Figure 2 (top right panel) shows the resulting map for Case 2 for comparison with Case 1 (left). We follow the same procedure as used by Vargas Domínguez (2010) to establish the direction of velocity vectors around the (naked) sunspot. Figure 2 (bottom panels) shows binary maps displaying the distinction between inward (white) and outward (black) radial components of the velocity vectors for Case 1 (left) and Case 2 (right) respectively. Our results agree with previous results for pore-like structures (Vargas Domínguez, 2010) showing that motions towards the pore are dominant in the closest vicinity. For Case 2 this behavior is even more evident and symmetric around the (naked) sunspot, showing the differential proper motions of plasma around the *anchored* spot. Motions at the periphery of the structure are significantly influenced by external plasma flows caused by exploding events as observed in previous works, for example, (Sobotka et al. 1999).

### 4. DISCUSSION, CRITICISM AND CONCLUSIONS

We remark that a moat and MMF activity could be considered as observed magnetic features, while the umbra and penumbra are observed intensity (or photometric) features. However we should not forget that this clas-

sification is based on the primary technique used for their identification, and several additional aspects of their nature should also be considered.

Figure 1 clearly shows a prominent horizontal magnetic component around the photometric naked sunspot. This horizontal component is co-spatial with the vertical component of the magnetic field in the outermost part of the photometric naked sunspot, and it persists as an horizontal magnetic structure beyond. This magnetic field configuration is very similar to that of a standard sunspot, at least from the magnetic point of view. That is, if we understand a sunspot as an intensity structure, the sunspot studied by ZETAL09 can be classified as a so-called *naked sunspot*. On the other hand, the configuration of the magnetic field resembles that of a sunspot with extended magnetic field beyond the penumbra (Sainz Dalda & Martínez Pillet 2005) and of a naked sunspot during the decay of a sunspot (Bellot Rubio et al. 2008). Sainz Dalda & Bellot Rubio (2008) using Hinode/NFI magnetograms sketched a possible scenario where the sea-serpent behavior of the more horizontal penumbral filaments explain the bipolar magnetic structures in the mid-penumbra that eventually become MMFs when they reach the moat. Both observations related the more horizontal magnetic field component of the sunspot with the MMF activity, in agreement with several observational and theoretical proposals (Harvey & Harvey 1973; Schlichenmaier 2002). In the data presented here, we observe a very similar magnetic field configuration, although the sunspot does not have a photometric penumbra. It has a very similar magnetic structure surrounding the naked sunspot, although without a filamentary distribution at the spatial resolution in these observations. The main conclusion presented by ZETAL09 was based on the observational evidence that the selected sunspot is a naked sunspot. That is true but only part of the story: only taking into account the intensity point of view, applying LCT without correcting for the inherent proper motion of the (naked) sunspot and focusing only on the proper motions of the surrounding granulation. In our analysis we have demonstrated that the apparent outflows from the naked spot are not actually moat flows (as suggested by ZETAL09), but rather the contribution from outward flows originating in the regular mesh of divergence centers around the pore, in agreement with previous results (e.g., Vargas Domínguez et al. 2010).

They did not take into account the whole, true magnetic configuration of the sunspot. They related an intensity feature (sunspot without penumbra) with a magnetic structure (MMF) only looking at the intensity and a magnetogram (i.e., longitudinal apparent magnetic flux map), neglecting to verify what the true magnetic topology of the sunspot was. Although ZETAL09 reported - probably for the first time - MMF activity around a naked sunspot, their suggested revision of the relationship between MMF activity and the extension of the more horizontal penumbral filaments on the moat can be questioned if one considers the true (vector) magnetic field of the naked sunspot. Does it mean that *all* MMF activity can be explained *uniquely* by the extension of the horizontal penumbral filaments in the moat or even by an horizontal component of the magnetic field around the naked sunspot? It does not, but the absence of a (photo-

metric) penumbra does not imply a lack of an horizontal field around naked sunspot, and therefore *some* MMF activity can still be explained by the current interpretation. So, the MMF of type I and III (see classification in Shine et al. 2000 and Figure 3 of Thomas et al. 2002) are compatible with the observed horizontal component around sunspots and (photometric) naked sunspots. We have shown how a (photometric) naked sunspot has associated a vertical and horizontal magnetic component slightly outside of its intensity edge and an horizontal magnetic component extending much further beyond its intensity edge. In this sense, the (magnetic) naked sunspot is a rather chaste sunspot.

## 5. ACKNOWLEDGMENTS

## REFERENCES

- Bellot Rubio, L. R., Tritschler, A., & Martínez Pillet, V. 2008, *ApJ*, 676, 698
- Brickhouse, N. S., & Labonte, B. J. 1988, *Sol. Phys.*, 115, 43
- Gosain, S., Tiwari, S. K., & Venkatakrisnan, P. 2010, *ApJ*, 720, 1281
- Harvey, K., & Harvey, J. 1973, *Sol. Phys.*, 28, 61
- Kosugi, T., Matsuzaki, K., Sakao, T., Shimizu, T., Sone, Y., Tachikawa, S., Hashimoto, T., Minesugi, K., Ohnishi, A., Yamada, T., Tsuneta, S., Hara, H., Ichimoto, K., Suematsu, Y., Shimojo, M., Watanabe, T., Shimada, S., Davis, J. M., Hill, L. D., Owens, J. K., Title, A. M., Culhane, J. L., Harra, L. K., Doschek, G. A., & Golub, L. 2007, *Sol. Phys.*, 243, 3
- Kubo, M., Ichimoto, K., Shimizu, T., Tsuneta, S., Suematsu, Y., Katsukawa, Y., Nagata, S., Tarbell, T. D., Shine, R. A., Title, A. M., Frank, Z. A., Lites, B., & Elmore, D. 2007, *PASJ*, 59, 607
- Meyer, F., Schmidt, H. U., Wilson, P. R., & Weiss, N. O. 1974, *MNRAS*, 169, 35
- Ravindra, B. 2006, *Sol. Phys.*, 237, 297
- Ruiz Cobo, B., & del Toro Iniesta, J. C. 1992, *ApJ*, 398, 375
- Sainz Dalda, A., & Bellot Rubio, L. R. 2008, *A&A*, 481, L21
- Sainz Dalda, A., & Martínez Pillet, V. 2005, *ApJ*, 632, 1176
- Schlichenmaier, R. 2002, *Astronomische Nachrichten*, 323, 303
- Sheeley, N. R. 1969, 9, 347
- Shine, R., Title, A., & Murdin, P. 2000, *Sunspots: Moving Magnetic Features and Moat Flow*
- Sobotka, M., Vázquez, M., Bonet, J. A., Hanslmeier, A., & Hirzberger, J. 1999, *ApJ*, 511, 436
- Thomas, J. H., Weiss, N. O., Tobias, S. M., & Brummell, N. H. 2002, *Astronomische Nachrichten*, 323, 383
- Tsuneta, S., Ichimoto, K., Katsukawa, Y., Nagata, S., Otsubo, M., Shimizu, T., Suematsu, Y., Nakagiri, M., Noguchi, M., Tarbell, T., Title, A., Shine, R., Rosenberg, W., Hoffmann, C., Jurcevic, B., Kushner, G., Levay, M., Lites, B., Elmore, D., Matsushita, T., Kawaguchi, N., Saito, H., Mikami, I., Hill, L. D., & Owens, J. K. 2008, *Sol. Phys.*, 249, 167
- Vargas Domínguez, S., Bonet, J. A., Martínez Pillet, V., Katsukawa, Y., Kitakoshi, Y., & Rouppe van der Voort, L. 2007, *ApJ*, 660, L165
- Vargas Domínguez, S., de Vicente, A., Bonet, J. A., & Martínez Pillet, V. 2010, *A&A*, 516, A91+
- Vargas Domínguez, S., Rouppe van der Voort, L., Bonet, J. A., Martínez Pillet, V., Van Noort, M., & Katsukawa, Y. 2008, *ApJ*, 679, 900
- Vrabc, D. 1971, in *IAU Symposium*, Vol. 43, *Solar Magnetic Fields*, ed. R. Howard, 329+
- Vrabc, D. 1974, in *IAU Symposium*, Vol. 56, *Chromospheric Fine Structure*, ed. R. G. Athay, 201+
- Zuccarello, F., Romano, P., Guglielmino, S. L., Centrone, M., Criscuolo, S., Ermolli, I., Berrilli, F., & Del Moro, D. 2009, *A&A*, 500, L5

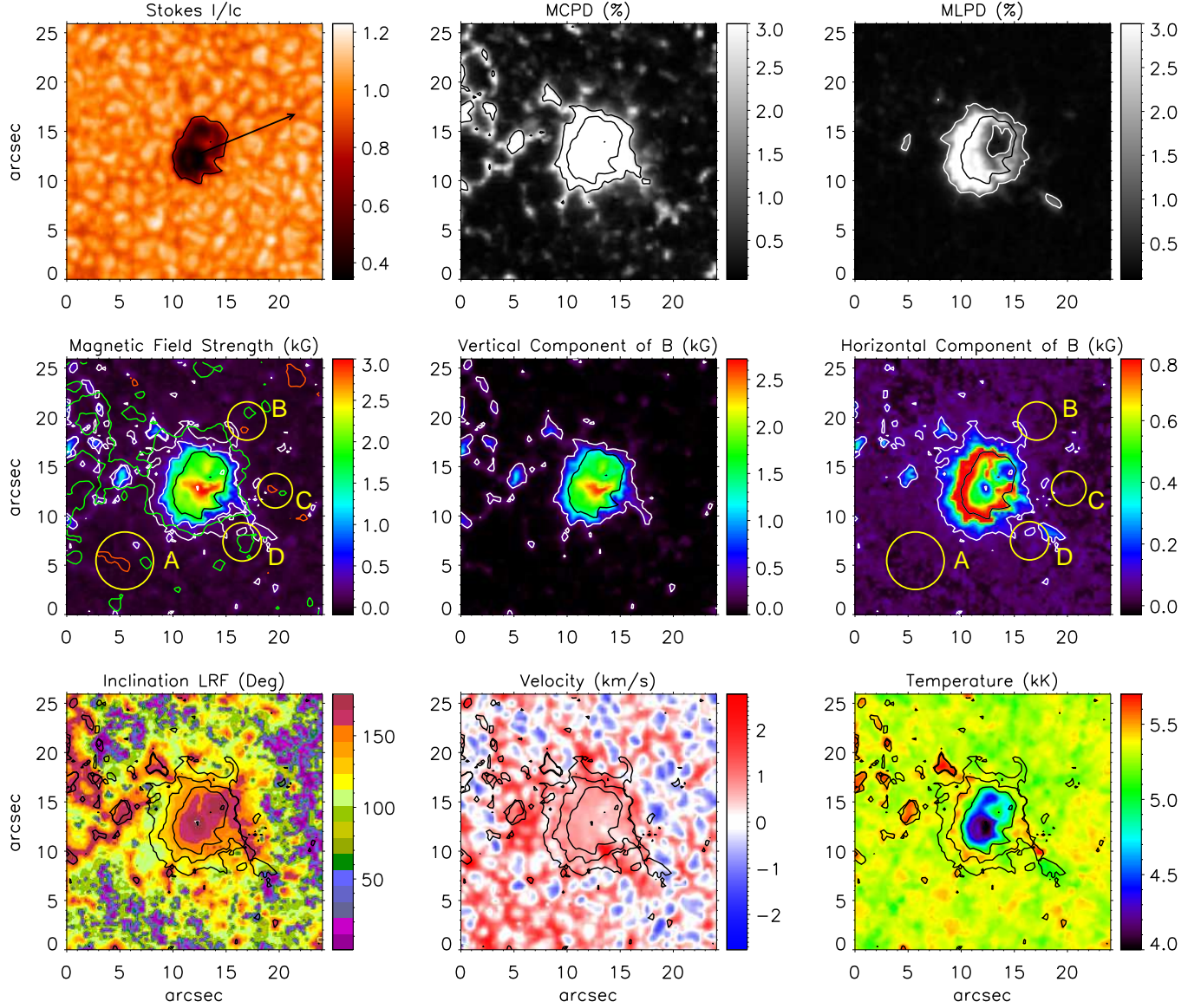


FIG. 1.— *Top panels:* intensity, mean circular polarization degree and mean linear polarization degree maps calculated directly from the Stokes parameters. *Bottom panels:* some physical values of the atmosphere obtained after the inversions done by SIR code. The second inner contour delimits the area mainly related with the vertical component of the magnetic field vector. The inner- and outermost contours delimit the horizontal component of the magnetic field vector.

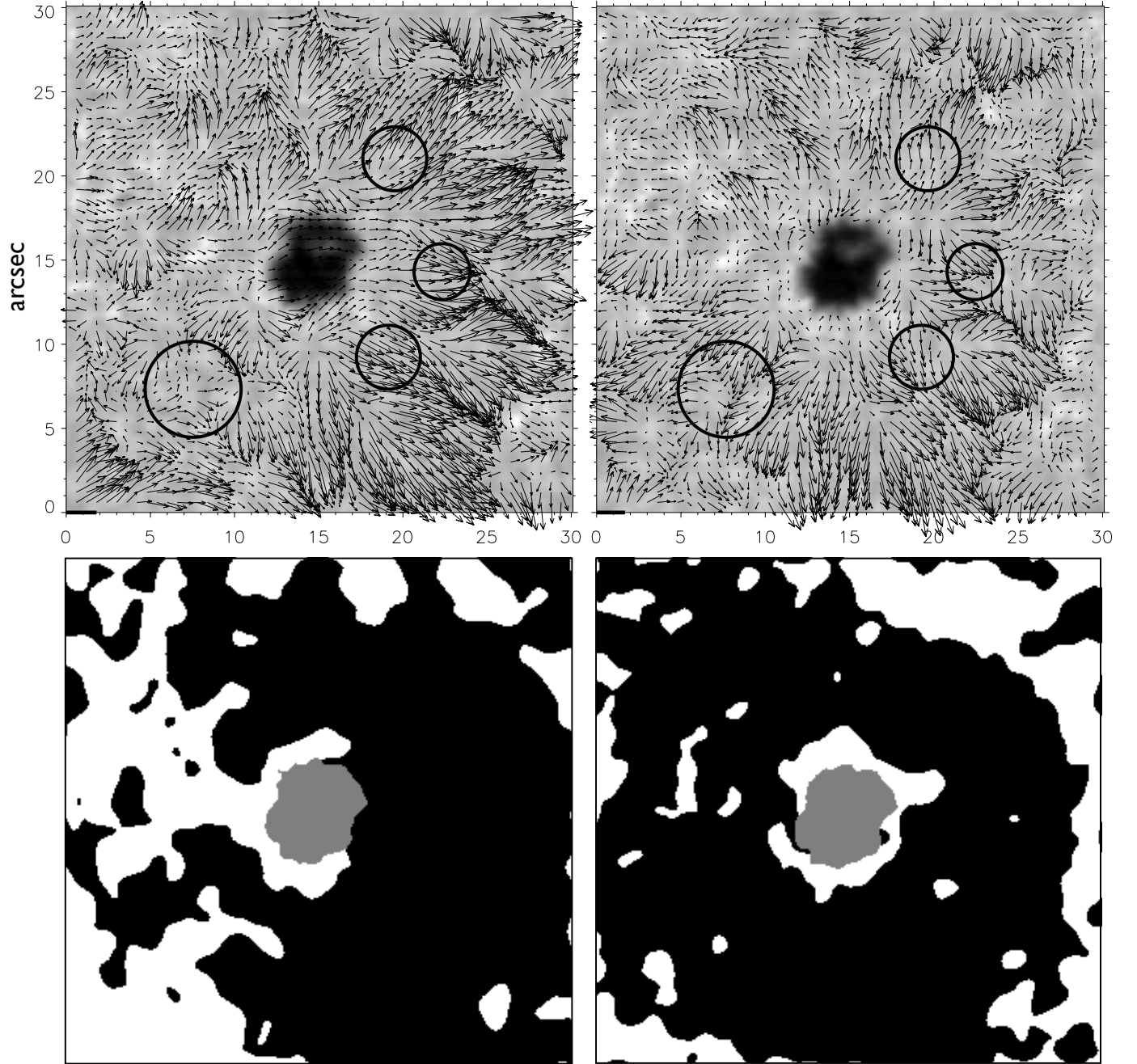


FIG. 2.— Distribution of horizontal proper motions around the naked (sunspot). *Top panels:* Maps of horizontal velocities for the *Hinode* (G-band) time series (92 min average) for Case 1 (left) and Case 2 (right). The background images represent the average image of the series. The length of the black bar at coordinates (0,0) corresponds to  $2 \text{ km s}^{-1}$ . *Bottom panels:* Binary maps of inward (white) and outward (black) radial velocity components for Case 1 (left) and Case 2 (right). See text for details.